Application of the Non-Intrusive Reduced Basis two-grid method on offshore wind farms

EMRSim 2022 Conference

Elise Grosjean [1]
Yvon Maday [1]

[1] Jacques-Louis Lions laboratory
Sorbonne Université

30.05.2022 - 02.06.2022

Purpose

Reduce the computational costs of offshore wind farms simulations with Non-Intrusive Reduced Basis methods

eDF

SAFRAN

C|T
ingenierie

CADLM
TRANSFORMING DATA INTO INTELLIGENCE

cemosis
Centre de modélisation et de simulation de Strasbourg

MINES ParisTech | PSL

Scilab

JJL

Introduction to the NIRB methods

Reduced basis methods

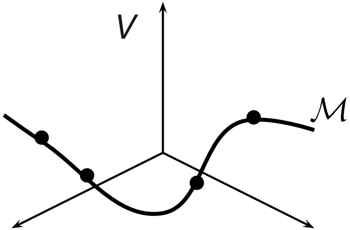

Figure: Solution manifold

$$\mathcal{M} = \{u(\mu) \in V |\ \mu \in \mathcal{G}\} \subset V.$$

- Parameter: $\mu \in \mathcal{G}$,
- Solution: $u(\mu) \in V$.

Introduction to the NIRB methods

Reduced basis methods

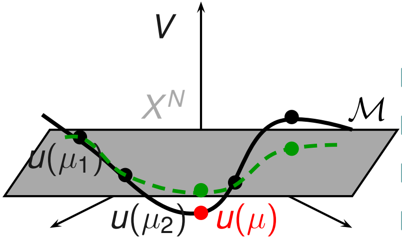

Figure: Solution manifold

$$\mathcal{M} = \{u(\mu) \in V |\ \mu \in \mathcal{G}\} \subset V.$$

- Parameters $\mu_1, \ldots, \mu_N \in \mathcal{G}$,
- Snapshots $u(\mu_1), \ldots, u(\mu_N) \in V_h$,
- X^N Reduced basis space,
- Projected snapshots onto X^N.

Introduction to the NIRB methods

Reduced basis methods

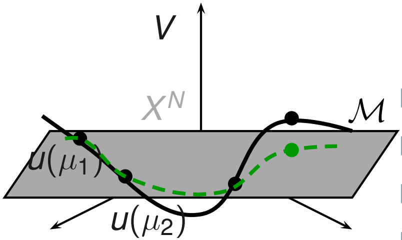

Figure: Solution manifold

$$\mathcal{M} = \{u(\mu) \in V | \ \mu \in \mathcal{G}\} \subset V.$$

$$\inf_{\dim(X^N)=N} \operatorname{dist}(\mathcal{M}, X^N).$$

- Parameters $\mu_1, \dots, \mu_N \in \mathcal{G}$,
- Snapshots $u(\mu_1), \dots, u(\mu_N) \in V$,
- X^N Reduced basis space,
- Projected snapshots onto X^N.

Kolmogorov n-width must be small [1] [2]

[1] P. Binev, A. Cohen, W. Dahmen, R. DeVore, G. Petrova, P. Wojtaszczyk *Convergence rates for greedy algorithms in reduced basis methods.* 2011.

[2] A. Buffa, Y. Maday, A.T. Patera, C. Prudhomme, and G. Turinici, *A Priori convergence of the greedy algorithm for the parameterized reduced basis.* 2012.

Introduction to the NIRB methods

Reduced basis methods

$$\mathcal{M}_h = \{u_h(\mu) \in V_h | \ \mu \in \mathcal{G}\} \subset V_h.$$

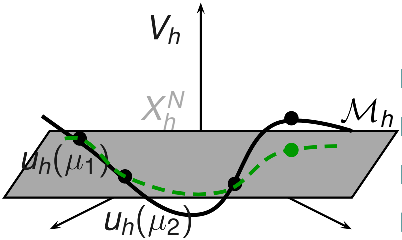

Figure: Solution manifold

- Parameters $\mu_1, \ldots, \mu_N \in \mathcal{G}$,
- Snapshots $u_h(\mu_1), \ldots, u_h(\mu_N) \in V_h$,
- X_h^N Reduced basis space,
- Projected snapshots onto X_h^N.

Kolmogorov n-width must be small [1] [2]

[1] P. Binev, A. Cohen, W. Dahmen, R. DeVore, G. Petrova, P. Wojtaszczyk *Convergence rates for greedy algorithms in reduced basis methods.* 2011.

[2] A. Buffa, Y. Maday, A.T. Patera, C. Prudhomme, and G. Turinici, *A Priori convergence of the greedy algorithm for the parameterized reduced basis.* 2012.

Introduction to the NIRB methods

Reduced basis methods

- Optimization over parameter space
- High Fidelity (HF) real-time simulations

Non-Intrusive Reduced basis methods (NIRB)

Industrial context $\rightarrow$ **black box solver**

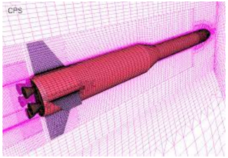

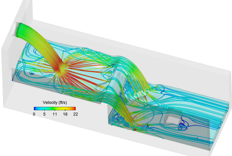

Application

Wind farm setting

Application

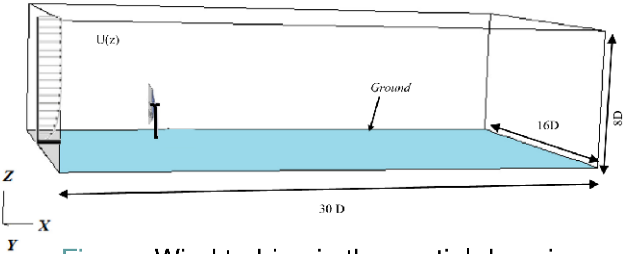

Figure: Wind turbine in the spatial domain

Application

- reference input velocity magnitude u_{ref}

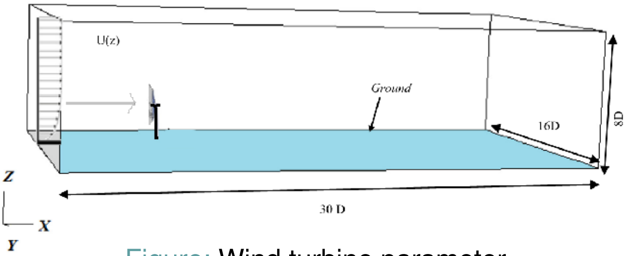

Figure: Wind turbine parameter

Application

- reference input velocity magnitude u_{ref}
- incidence angle θ

Figure: Wind turbine parameter

Actuator disc [3] and $k - \varepsilon$ RANS equations

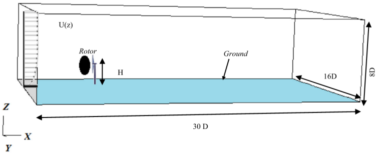

Figure: Rotor

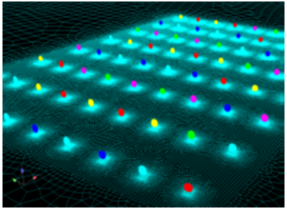

Figure: Wind farm with actuator discs, image from EDF.

[3] Sumner, J. and España, G. and Masson, C. and Aubrun, S. *Evaluation of RANS/actuator disk modelling of wind turbine wake flow using wind tunnel measurements.* 2013.

Actuator disc and $k - \varepsilon$ RANS equations

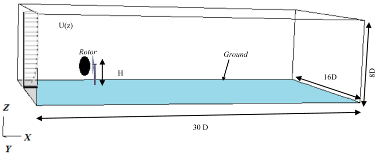

Figure: Rotor

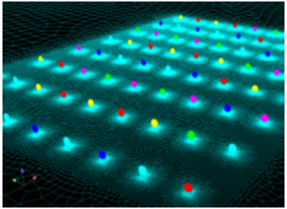

Figure: Wind farm with actuator discs, image from EDF.

EDF SALOME CODE SATURNE

NIRB approach

The NIRB two-grid method is applied to approximate a quasi-stationary state.

NIRB approach [5] [6] [7]

$$\mathcal{P} : (u_{ref}, \theta) \to u^F,$$

with u^F: velocity inside the actuator disc at final time.

- $u^F(\mathbf{x}; u_{ref}, \theta)$: Unknown
  - $u_h^F \in V_h$ on a fine mesh $\mathcal{T}_h$ (HF),
  - $u_H^F \in V_H$ on a coarse mesh $\mathcal{T}_H$.

1. Offline stage: $u_h^F((u_{ref}, \theta)_i)$: Snapshots on $\mathcal{T}_h \quad (\in X_h^N)$
2. Online stage: $u_H^F(u_{ref}, \theta)$: Solution on $\mathcal{T}_H \quad (H^2 \sim h)$

[5] R. Chakir, Y. Maday, *A two-grid finite-element/reduced basis scheme for the approximation of the solution of parameter dependent PDE.* 2009.

[6] E. Grosjean, Y. Maday, *error estimate of the non-intrusive reduced basis method with finite volume schemes.* 2021.

[7] E. Grosjean, Y. Maday, *Error estimate of the Non-Intrusive Reduced Basis (NIRB) two-grid method with parabolic equations.* 2022.

Decomposition

Separation of variables

$$u_h(\mathbf{x}; u_{ref}, \theta) = \sum_{j=1}^{N} a_j^h(u_{ref}, \theta)\, \Phi_j^h(\mathbf{x}),$$

$(\Phi_j^h)_{j=1,\dots,N} \in X_h^N$: L^2-orthonormalized basis functions (modes)

Coefficients $a_j^h(u_{ref}, \theta)$

- Optimal coefficients: $(u_h^F(u_{ref}, \theta), \Phi_j^h(\mathbf{x}))$,
- Our choice: $(u_H^F(u_{ref}, \theta), \Phi_j^h(\mathbf{x}))$, with $(\Phi_j^h)_{j=1,\dots,N}$ L^2 & H^1-orthogonalized

$\mu = (u_{ref}, \theta)$

NIRB – OFFLINE/ONLINE

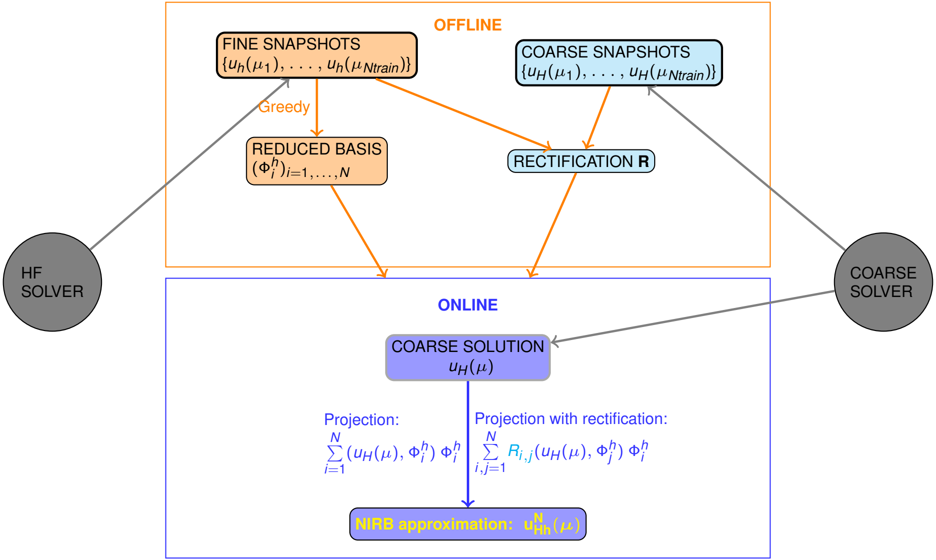

Post-treatment

Post-Treatment: The rectification method [4]

$(u_H^i, \Phi_j) \to (u_h^i, \Phi_j)$

$$(A_i)_k = (u_H(\mu_k), \Phi_i)_{L^2}, \forall k = 1, \cdots, Ntrain$$
$$(B_i)_k = (u_h(\mu_k), \Phi_i)_{L^2}, \forall k = 1, \cdots, Ntrain$$
$$D = (A_1, \cdots, A_N) \in \mathbb{R}^{Ntrain \times N}$$

$$\boxed{R_i = (D^T D + \lambda I_N)^{-1} D^T B_i, \ \forall i = 1, \cdots, N.}$$

$$u_{Hh}^N(\mu) = \sum_{i,j=1}^{N} R_{ij}(u_H(\mu), \Phi_j)\Phi_i$$

[4] Rachida Chakir, Yvon Maday,Philippe Parnaudeau. *Non Intrusive RB for Heat transfer* 2018

2D & 3D results

Wind turbines results

One application: 2D Wind turbine

- Turbine power $P = c_P \frac{1}{2} \rho A u_*^3$,

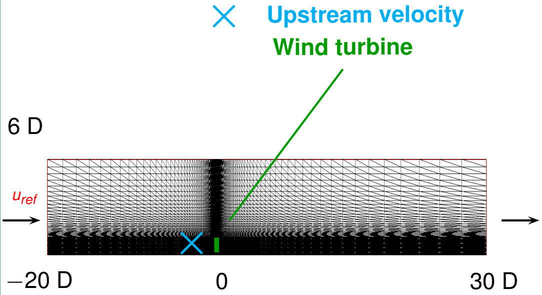

Figure: Mesh for one wind turbine

One application: 2D Wind turbine

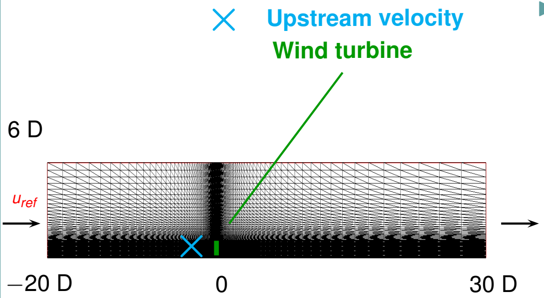

Figure: Mesh for one wind turbine

- Turbine power $P = c_P \frac{1}{2} \rho A u_*^3$,
- c_P: Power coefficient, ρ: wind density, A: disc area,

u_{ref}: Variable parameter

One application: 2D Wind turbine

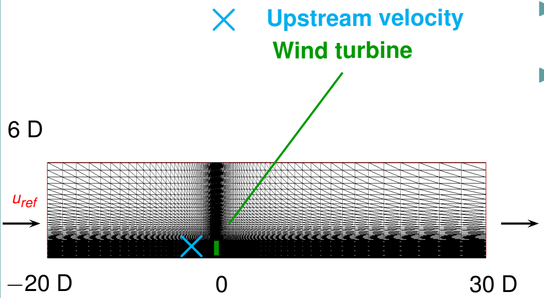

Figure: Mesh for one wind turbine

- Turbine power $P = c_P \frac{1}{2}\rho A u_*^3$,
- c_P: Power coefficient, ρ: wind density, A: disc area,
- u_*: velocity upstream the wind turbine,

u_{ref}: Variable parameter

One application: 2D Wind turbine

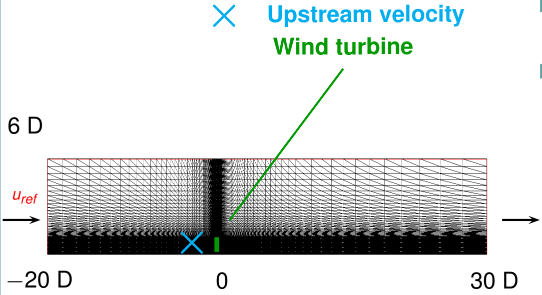

Figure: Mesh for one wind turbine

- Turbine power $P = c_P \frac{1}{2} \rho A u_*^3$,
- c_P: Power coefficient, ρ: wind density, A: disc area,
- u_*: velocity upstream the wind turbine,

Wind simulation

- 2D mesh with 6500 cells, refined around the wind turbine.
- Rotor diameter: D=150m
- Hub height: 95.6m.
- Zooms around the probes (upstream the turbine)
- Zooms around the turbines

One application: 2D Wind turbine

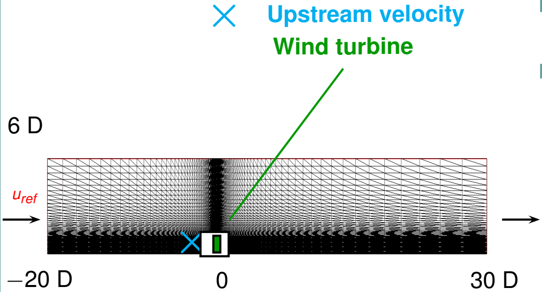

Figure: Mesh for one wind turbine

- Turbine power $P = c_P \frac{1}{2}\rho A u_*^3$,
- c_P: Power coefficient, ρ: wind density, A: disc area,
- u_*: velocity upstream the wind turbine,

Wind simulation

- 2D mesh with 6500 cells, refined around the wind turbine.
- Rotor diameter: D=150m
- Hub height: 95.6m.
- Zooms around the probes (upstream the turbine)
- Zooms around the turbines

One application: 2D Wind turbine

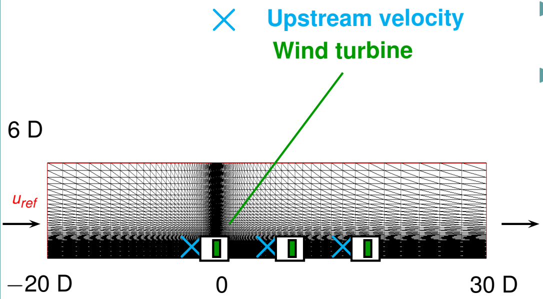

Figure: Mesh for one wind turbine

- Turbine power $P = c_P \frac{1}{2} \rho A u_*^3$,
- c_P: Power coefficient, ρ: wind density, A: disc area,
- u_*: velocity upstream the wind turbine,

Wind simulation

- 2D mesh with 6500 cells, refined around the wind turbine.
- Rotor diameter: D=150m
- Hub height: 95.6m.
- Zooms around the probes (upstream the turbine)
- Zooms around the turbines

One application: 2D Wind turbine

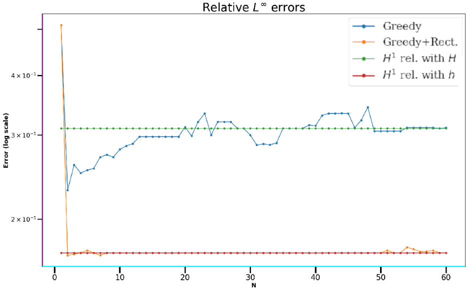

Figure : L^∞ relative errors between the reference solution and u_{Hh}^N (with and without rectification P-T), Ntrain=66, u_{ref} = 10.5, on the probe

- Turbine power $P = c_P \frac{1}{2}\rho A u_*^3$,
- c_P: Power coefficient, ρ: wind density, A: disc area,
- u_*: velocity upstream the wind turbine,

Wind simulation

- 2D mesh with 6500 cells, refined around the wind turbine.
- Rotor diameter: D=150m
- Hub height: 95.6m.
- Zooms around the probes (upstream the turbine)
- Zooms around the turbines

3D application

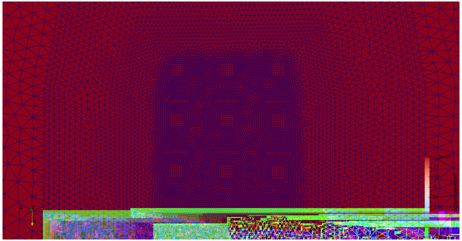

Figure: Wind turbines

3D application

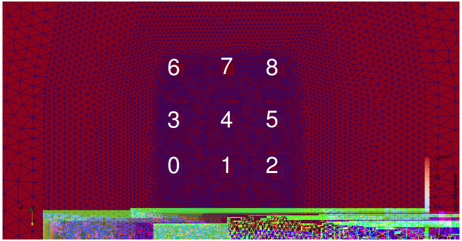

Figure: Wind turbines

3D application

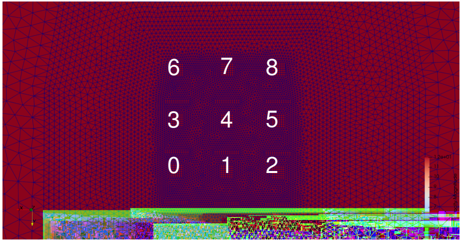

Figure: Wind turbines

Parameter: Wind magnitude & incidence angle

3D application

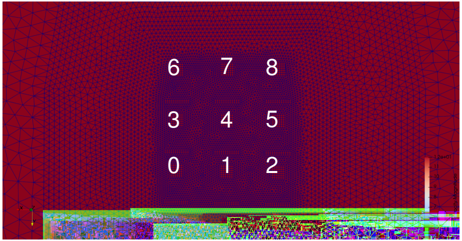

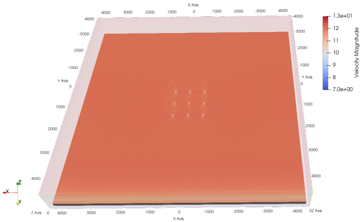

Figure: Wind turbines

Parameter: Wind magnitude & incidence angle

3D mesh

Nodes for one turbine	Fine mesh	Coarse mesh
	451 716	57 676

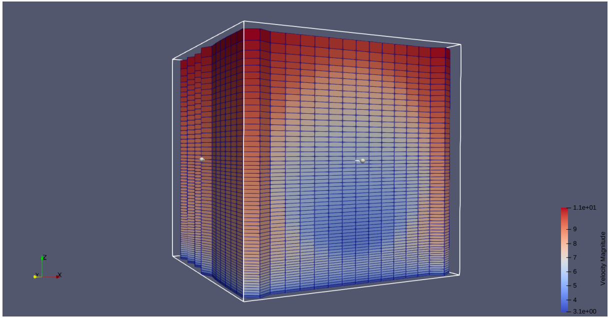

Figure: Wind around the turbine

Computational costs (min:sec)	Fine mesh	Coarse mesh
	40:00	03:00

3D results

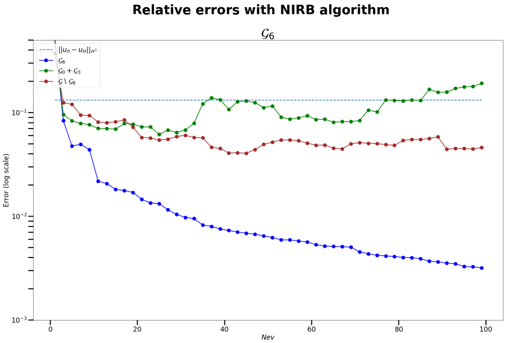

Figure: Wind turbine (Leave-one-out)

Offline NIRB + rectification $N = 20$ (h:min)	Online NIRB (h:min)
15:10	00:05

3D results

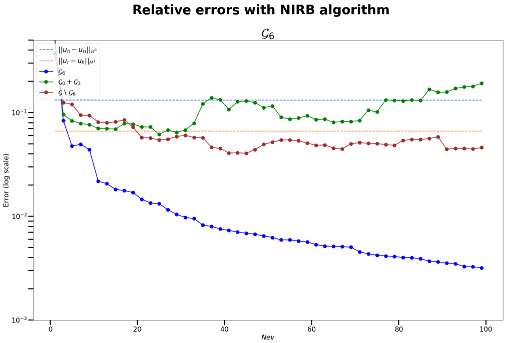

Figure: Wind turbine (Leave-one-out)

Offline NIRB + rectification $N = 20$ (h:min)	Online NIRB (h:min)
15:10	00:05

Conclusions & Perspectives

- Several applications with offshore wind farms: Accurate approximations with computational costs of coarse solutions
- Development of two new NIRB tools

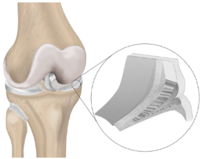

TECHNISCHE UNIVERSITÄT KAISERSLAUTERN

Figure: Meniscus tissue

Perspectives

- Two-grid a-posteriori error estimates
- Tests 5×5 wind farm with the new NIRB methods

Thank you for your attention!

TECHNISCHE UNIVERSITÄT KAISERSLAUTERN

SORBONNE UNIVERSITÉ

EDF

Elise Grosjean

NIRB – OFFLINE/ONLINE

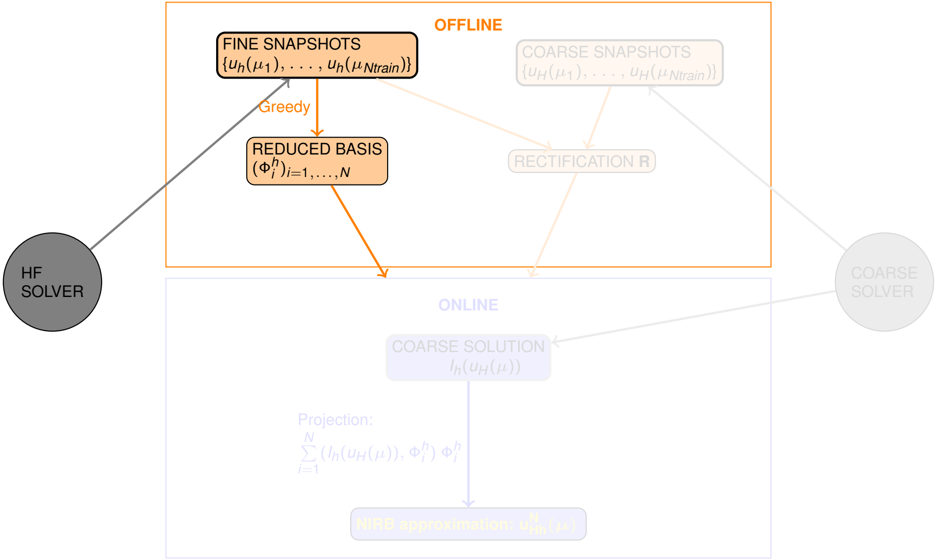

NIRB – OFFLINE/ONLINE

Greedy algorithm

$\rightarrow L^2$ orthonormalization.

+ Eigenvalue problem: $\forall v \in X_h^N, \int_\Omega \nabla \Phi_h \cdot \nabla v = \lambda \int_\Omega \Phi_h \cdot v$

$\rightarrow L^2(\Omega)$ and $H^1(\Omega)$ orthogonalization.

$$\mathbf{X_h^N} = \mathbf{Span}\{\mathbf{\Phi}_1^h, \ldots, \mathbf{\Phi}_N^h\}$$

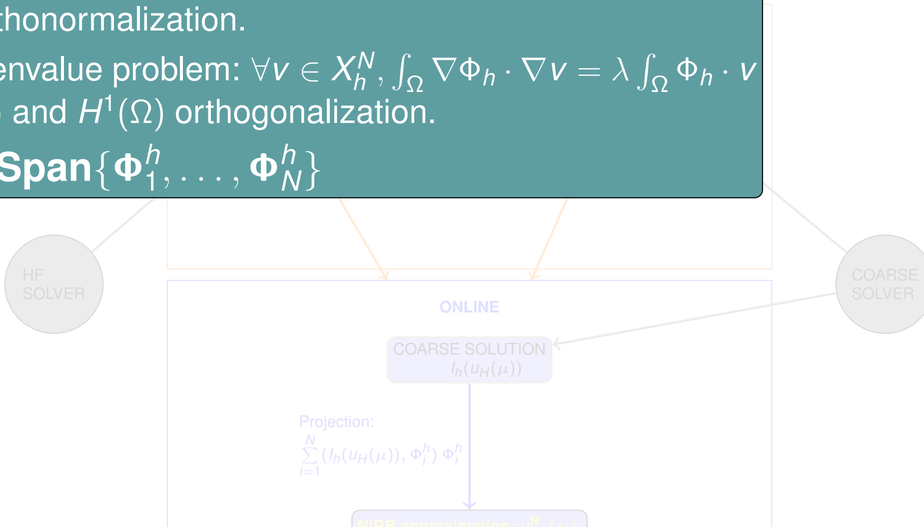

NIRB – OFFLINE/ONLINE

Greedy algorithm

$\rightarrow$ L^2 orthonormalization.

$+$ Eigenvalue problem: $\forall v \in X_h^N, \int_\Omega \nabla \Phi_h \cdot \nabla v = \lambda \int_\Omega \Phi_h \cdot v$

$\rightarrow$ $L^2(\Omega)$ and $H^1(\Omega)$ orthogonalization.

$$\mathbf{X_h^N} = \mathbf{Span}\{\mathbf{\Phi}_1^h, \ldots, \mathbf{\Phi}_N^h\}$$

HF SOLVER

COARSE SOLVER

ONLINE

COARSE SOLUTION $I_h(u_H(\mu))$

Projection: $\sum_{i=1}^{N} (I_h(u_H(\mu)), \phi_i^h)$

× **Greedy**

for $n = 1, \ldots, N$:

$$\widetilde{\mu}_n = \arg\max_{\mu \in \mathcal{G}} \frac{\left\| u_h(\mu) - P^{n-1}(u_h(\mu)) \right\|}{\left\| u_h(\mu) \right\|}$$

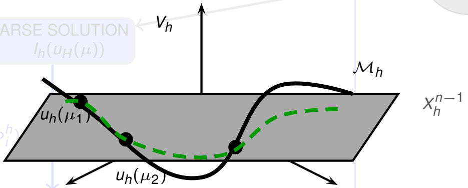

NIRB – OFFLINE/ONLINE

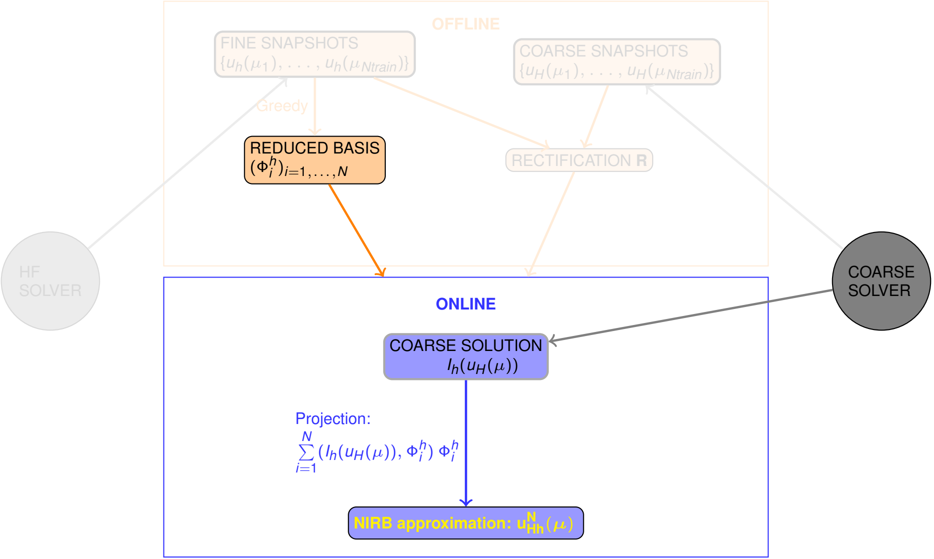

NIRB – OFFLINE/ONLINE

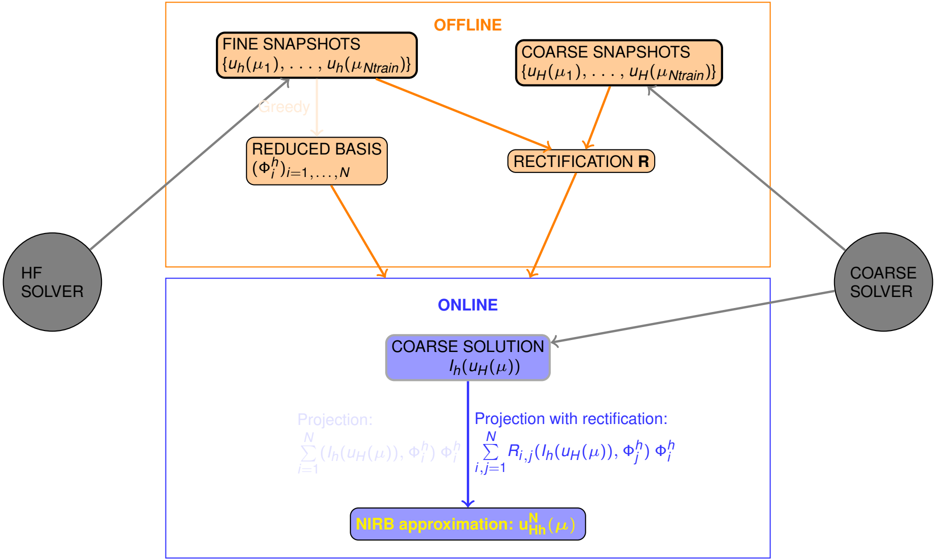

3D Results

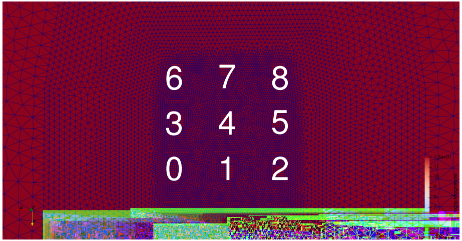

Figure: 3×3 turbines

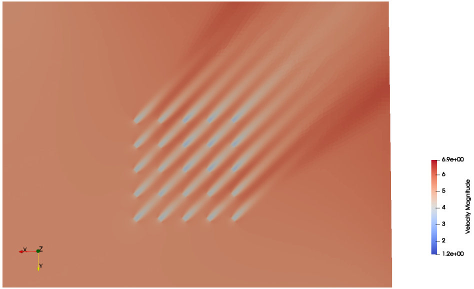

Figure: 5×5 turbines

3D Results

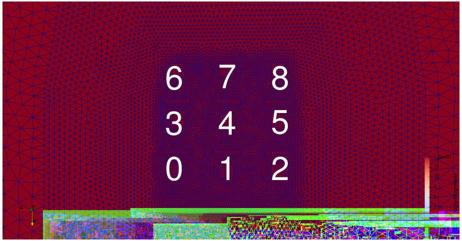

Figure: 3 $\times$ 3 turbines

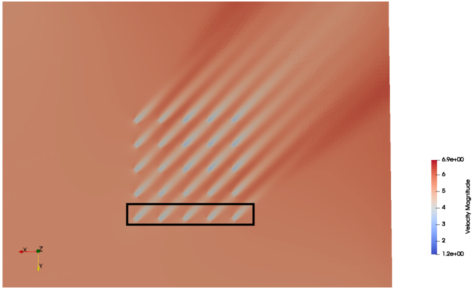

Figure: 5 $\times$ 5 turbines

3D Results

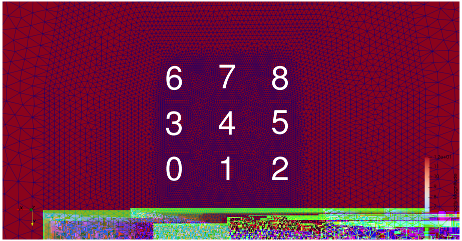

Figure: 3 × 3 turbines

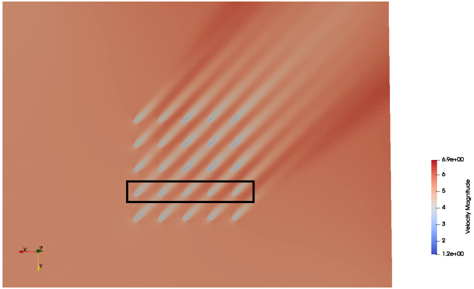

Figure: 5 × 5 turbines

3D Results

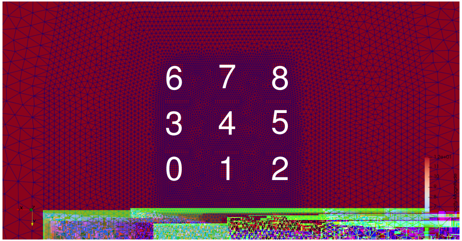

Figure: 3×3 turbines

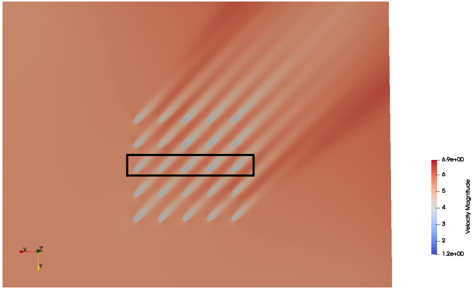

Figure: 5×5 turbines

3D Results

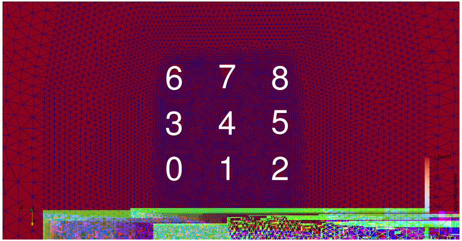

Figure: 3 × 3 turbines

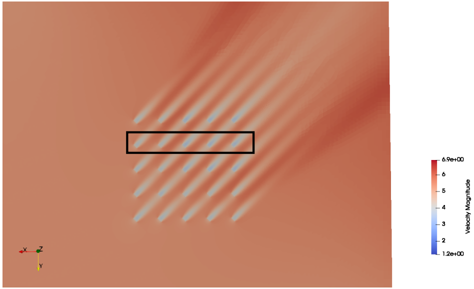

Figure: 5 × 5 turbines

3D Results

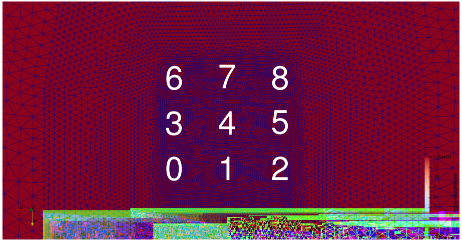

Figure: 3 × 3 turbines

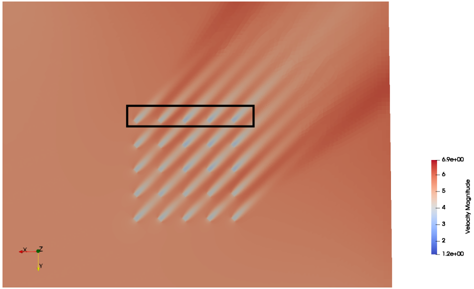

Figure: 5 × 5 turbines

3D results

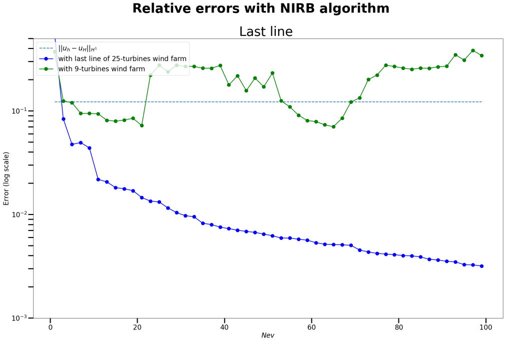

Figure: Wind turbines (Leave-one-out)

3D results

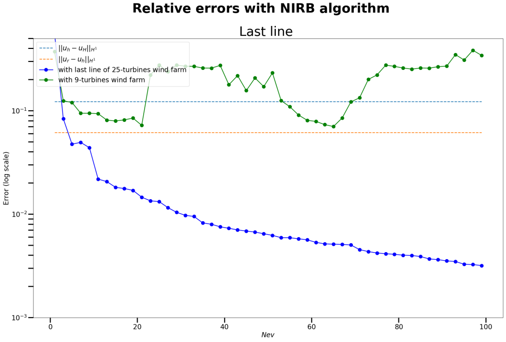

Figure: Wind turbines (Leave-one-out)

More results

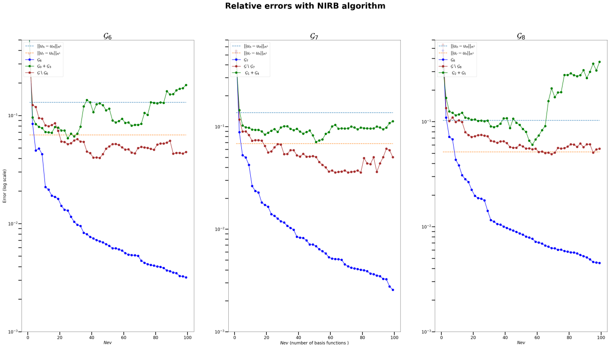

Figure: Wind turbines

RANS

- $u = (u_1, u_2, u_3)$: wind velocity,
- p: wind pressure,
- ρ: density,
- μ: dynamic viscosity.
- Reynolds tensor: $\overline{u_i' u_j'}$,
- $\overline{F}$: additional source terms.

$$\begin{cases} \frac{\partial \rho}{\partial t} + \frac{\partial(\rho \overline{u}_i)}{\partial x_i} & = 0, \\ \frac{\partial \overline{u}_i}{\partial t} + \overline{u}_j \frac{\partial \overline{u}_i}{\partial x_j} & = -\frac{1}{\rho}\frac{\partial \overline{p}}{\partial x_i} + \frac{\partial}{\partial x_j}(\mu(\frac{\partial \overline{u}_i}{\partial x_j} + \frac{\partial \overline{u}_j}{\partial x_i}) - \frac{1}{\rho}\overline{u_i' u_j'}) + \overline{F}, \end{cases}$$